



Reaction runaway as a domino effect of pool fire engulfing an ethoxylation reactor

Federico Florit, Valentina Busini*, Simone Favrin, Renato Rota, Marco Derudi

Politecnico di Milano, Piazza Leonardo da Vinci, 32, Milan, Italy

*valentina.busini@polimi.it

In industrial safety, engulfing pool fires can cause damages and collapse of process vessels with catastrophic consequences. This work investigates the ethoxylation of 1-dodecanol as a case-study with a multiscale approach able to analyse scenarios of runaway triggered by a pool fire engulfing the reactor. The aim is to understand whether and when the cooling power of the external heat exchanger can prevent dangerous temperature build-up in the chemical reactor.

1. Introduction

Pool fires impinging a reactor may trigger an explosion due to reaction runaway or pressure rise, in particular when they engulf the reactor. The domino effect could be more hazardous than the pool fire itself, so a prompt evaluation of the situation for the planning of emergency intervention is of paramount importance.

Experimental works are available about the average heat flux over the surface of packages for the transport of high-level radioactive material (Feldkamp et al., 2020) or the ability of tank cars to meet thermal protection requirements under conditions of total containment (i.e., no pressure relief devices) (Gonzalez et al., 2016). More recent works used the computational fluid dynamics (CFD) for the prediction of the behaviour of pressurized tanks fully (Scarponi et al., 2019) or partially engulfed in pool fire (Scarponi et al., 2021). In case of reaction runaway, the CFD modelling of complex fluid-dynamics and reactivity effects inside the vessel could be impractical because of the extremely turbulent conditions coupled with reaction in a multi-phase system. For these reasons, in this work, the union of CFD and 0D model is presented as a valid and simple tool for the safety assessment of fire accidental scenarios.

A reactor engulfed by fire was considered, studying the effect of the pool fire dimensions on the possible runaway triggered by the external heating with the aim to understand whether and when the cooling power of the external heat exchanger can prevent dangerous temperature build-up in the chemical reactor. The multiscale approach used in this work involves a series of mathematical simulations able to evaluate the effects of different pool fires in terms of heat flux entering the reactor. These simulations were carried out using the computational fluid dynamics. The results of such simulations were used to carry out a parametric study, with a 0D model able to foresee the dynamic behaviour of the reactor engulfed in the pool fire, which also produced a practical instrument for making an estimation of the time available for activating proper mitigation measures.

2. Case study

An industrial Venturi Loop Reactor (VLR) for the ethoxylation of 1-dodecanol is chosen as a case study. The reactor is a hemispherically capped tank equipped with an ejector and an external heat exchanger, as depicted in Figure 1. A given quantity of dodecanol is charged into the reactor (within a nitrogen atmosphere), the recirculation pump is activated, and an ethylene oxide (EO) stream is fed into the reactor at a constant flowrate via a gas line from a storage tank. Together with EO, nitrogen is also fed into the reactor with a known flowrate, as the EO storage tank is generally padded with this gas. The VLR is quite large on industrial scale, having a height of up to 9 m and a height-to-diameter ratio ranging from 2 to 3.

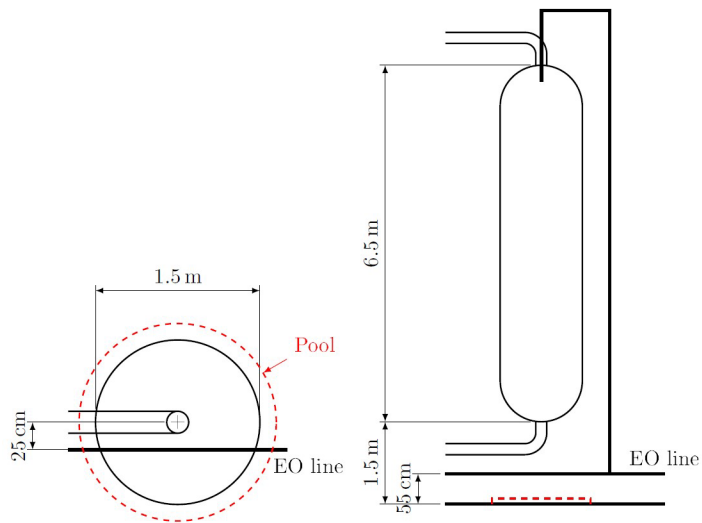


Figure 1: Diagram of the ethoxylation reactor.

This reactor configuration is affected by several intrinsic hazards, as the involved reaction of ethoxylation is exothermic (accounting for a reaction enthalpy of about -92 kJ/mol), the involved quantities are large (tons of material), and all the chemicals are flammable and/or toxic. The typical reaction temperature is about 180 °C, which can be obtained as a pseudo-steady temperature inside this fed-batch reactor by properly controlling the cooling effect of the external heat exchanger. The reactor/heat-exchanger configuration and the operating conditions are reported in Table 1, reporting the reactor radius, R , the reactor height, H , the heat exchanger transfer coefficient multiplied by the exchange area, US , the initial dodecanol mass, m_0 , and the initial temperature, T_0 .

Table 1: Dimensions of the VLR, heat exchanger characteristics, and operating conditions.

R [m]	H [m]	US [W/K]	m_0 [kg]	T_0 [°C]
0.75	6.5	40,000	2,000	160

The reactions involved in the system are the ethoxylation process (happening in the liquid phase, forming fatty alcohol ethoxylates from dodecanol and the dissolved EO) (Di Serio et al., 2005; Florit et al., 2019) and the undesired decomposition of ethylene oxide (within the gaseous phase, producing methane and carbon monoxide, with a reaction enthalpy of about -132 kJ/mol) (Crocco et al., 1959). The decomposition reaction is triggered at high temperatures (as the activation energy of such reaction is large), especially when the concentration of EO is large; this condition may happen when an external fire heats the reactor. A fire can occur because of a leak from the reactor, leading to a pool of flammable, low-boiling liquids underneath the vessel. This accidental scenario will be considered, studying the effect of the pool fire dimensions on the possible runaway triggered by the external heating (domino effect) which may be not compensated by the heat exchanger. The pool is assumed to be centred with respect to the reactor, on the ground, and thus at 1.5 m from the bottom of the vessel. Given the large amount of material involved in the vessel, different leaks can lead to pools having very diverse diameters.

3. Pool fire CFD analysis

The pool fire originating from the leak can be modelled using CFD, to describe the extent and the heat release rate (HRR) of the flame (Tavelli et al., 2013). Fire Dynamics Simulator (FDS) software from NIST (McGrattan et al., 2013) was chosen for this work.

The pool underneath the reactor was simulated using the properties of dodecane (FDS library) as a proxy of those of dodecanol and the ethoxylation products in terms of physical-chemical properties pertaining fire simulations. Different simulations were run to consider different leaks, leading to different pool diameters, ranging from 0.5 to 2.0 m. The diameter of the pool is assumed constant over time; these simulations correspond also to different catch basin dimensions, if one is present under the reactor.

Similarly to what was done in a previous work on jet-fire impingement (Florit et al., 2019), in the simulation the reactor is equipped with four vertical rows of sensors to record the heat flux on the surface of the VLR at different

heights. The total heat flux due to pool fire engulfment is computed from the contribution of all sensors. An example result for a pool of radius 1.25 m is reported in Figure 2a, where the total heat flux is reported as a function of time. Notably, the heat flux reaches a steady value after approximately 10 s (this was observed in all simulations) and can thus be represented by its average (dashed line in the figure) over time.

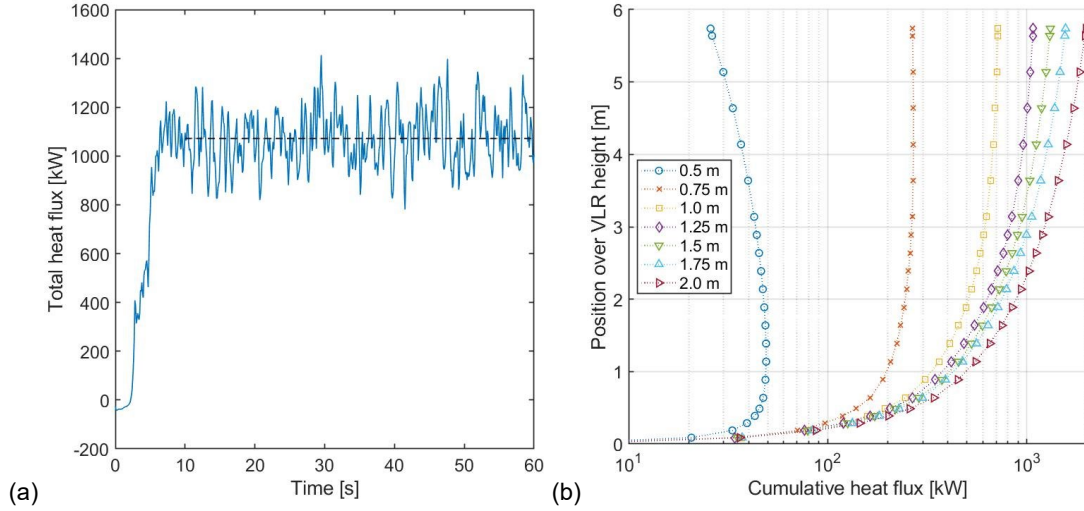


Figure 2: (a) Total heat flux entering the VLR due to a pool fire of 1.25 m radius. (b) Cumulative heat flux along reactor height for different pool radii.

Instead, by observing the averaged heat flux at each position over the height of the VLR, it is possible to determine whether the reactor can be considered engulfed or partially engulfed. Figure 2b reports the cumulative heat flux along the reactor height, thus the value obtained at the top of the reactor corresponds to the total average heat flux reported in Figure 2a. Notably, the cumulative flux is monotonically increasing for all pools having a radius greater than the reactor radius; while, pools having a radius equal or lower than the VLR one have a cumulative heat flux that is constant (no heat gain) or decreasing (cooling by the external environment) after a certain height (e.g., roughly 4 m for the pool of 0.75 m radius, and 1 m for the pool of 0.5 m radius). Therefore, the VLR can be considered engulfed by pool fires having a pool radius larger than the reactor radius, and partially engulfed (or impinged) otherwise.

4. 0D model for runaway

The Maximum Allowable Temperature (MAT) inside the system can be used to define whether the reactor has reached a critical safety condition (Copelli et al, 2011a, 2011b) for the presence of the external fire heating the vessel. The MAT is chosen to be equal to the EO critical temperature (196 °C). EO solubility decreases at increasing temperature (Di Serio et al., 2005), thus a build-up of hazardous gas is happening when the EO critical temperature is exceeded. This can possibly trigger the unwanted decomposition reaction of EO in the gas phase, leading to the vessel pressurization and burst (if no protection is in place). The proper modelling of the VLR can help predicting whether the MAT is exceeded according to the external flame heat flux.

The VLR can be considered a well-mixed system due to the presence of the ejector, which guarantees a high degree of mixing between the gas and the liquid phases. Physical-chemical properties (for each phase) and temperature (equal for both phases) can be considered uniform. Macroscopic balance equations can thus be used to model the time evolution of this kind of reactor.

Species mass balances are required to compute the reactor composition. For the gaseous phase:

$$\frac{dn_i^G}{dt} = F_i - \phi_i + R_i^G V_G \quad (1)$$

where n_i^G is the number of moles of species i in the gas, F_i the molar gaseous feed rate of species i , ϕ_i species i molar flux due to condensation, R_i^G the molar production rate of species i due to gaseous phase reactions, and V_G the gas volume. For the liquid phase:

$$\frac{dn_i^L}{dt} = \phi_i + R_i^L V_L \quad (2)$$

where n_i^L is the number of moles of species i in the liquid, R_i^L the molar production rate of species i due to liquid phase reactions, and V_L the liquid volume (calculated assuming ideal mixtures). The total reactor volume will be equal to $V_r = V_G + V_L$.

Using a global energy balance, involving both the reactor and the external heat exchanger, under the assumption of ideal mixtures the following equation arises:

$$\begin{aligned} \sum_{i=1}^{NC} (n_i^G \tilde{c}_{p,i}^G + n_i^L \tilde{c}_{p,i}^L) \frac{dT}{dt} \\ = \sum_{i=1}^{NC} F_i \tilde{c}_{p,i}^G (T_{IN} - T) + \sum_{i=1}^{NC} \phi_i \Delta \tilde{h}_i^{ev} - \sum_{j=1}^{NRG} \Delta \tilde{H}_{R,j}^G r_j^G V_G - \sum_{j=1}^{NRL} \Delta \tilde{H}_{R,j}^L r_j^L V_L + \dot{Q}_{HE} + \dot{Q}_f \end{aligned} \quad (3)$$

where $\tilde{c}_{p,i}^G$ and $\tilde{c}_{p,i}^L$ are species i molar specific heat capacities in the two phases, T the reactor temperature, T_{IN} the feed inlet temperature, $\Delta \tilde{h}_i^{ev}$ the molar enthalpy of evaporation, NRG and NRL the number of reactions in the gas and the liquid, $\Delta \tilde{H}_{R,j}^G$ and $\Delta \tilde{H}_{R,j}^L$ the molar reaction enthalpies for reaction j in the gas and liquid phase, r_j^G and r_j^L the j -th reaction rates in the two phases, \dot{Q}_{HE} the heat exchanger duty, and \dot{Q}_f the inlet heat flux due to presence of the external fire. For how the model is built, the term \dot{Q}_f can be used to consider the effect of a flame engulfing the reactor (i.e., for the scenario considered in this work), or the heat exchanger (e.g., because of the recirculation loop leaking and forming a pool underneath the heat exchanger), or both.

The condensation flux can be assumed to be proportional to a concentration difference between the gas phase bulk and the gas-liquid interface, where phase equilibrium is established:

$$\phi_i = k_L a (c_i^{bL} - c_i^{eqL}) V_L \quad (4)$$

where k_L is the liquid mass transfer coefficient, a the bubble surface per unit volume, c_i^{bL} the bulk molar concentration of species i in the liquid phase, and c_i^{eqL} the equilibrium concentration (solubility) of species i in the liquid. Generally, for VLR ejectors $k_L a = 0.2 \div 1.5 \text{ s}^{-1}$ (Di Serio et al., 2005). Solubilities can be determined using thermochemical data and, in the simplest case, the Raoult's law.

The heat exchanger duty can be computed, assuming that the coolant has uniform and constant temperature (which is a reasonable assumption considering that the exchanger is not hit by flames and that the power/cooling control system is adequate to keep the temperature constant), T_{cool} , and the reaction influence is negligible inside the heat exchanger:

$$\dot{Q}_{HE} = F_{circ} \tilde{c}_p^{avg} (T - T_{cool}) \left(1 - \exp \left(- \frac{USF_{circ}}{\tilde{c}_p^{avg}} \right) \right) \quad (5)$$

where U is the global heat exchange coefficient, S the heat exchange surface, F_{circ} the circulating molar flowrate and \tilde{c}_p^{avg} the average specific heat capacity inside the VLR.

The parameter \dot{Q}_f is described as a constant heat flux (as the flame can be considered steady after a time that is way lower than the reaction time), acting on the reactor for a given duration, Δt_f , and starting from a time t_f^0 within the process time. By fixing the flame heat flux and parametrically changing the value of the other two quantities, the time required to reach the MAT can be computed. This time corresponds to the flame duration able to increase the reactor temperature up to the MAT. Figure 3 is obtained, depicting the time needed to reach the MAT (corresponding to the flame duration) according to the time at which the flame starts engulfing the reactor, for fires providing different inlet powers. Times below each curve represent safe conditions, as the MAT is never reached during the fire scenario, while times equal or above the curve represent conditions for which the MAT is exceeded. The minimum of such a curve is the minimum flame duration which leads to unsafe conditions inside the reactor, therefore corresponding to the maximum time allowed to take some countermeasures (maximum intervention time). For example, a flame with a HRR of 600 kW flame can lead to unsafe conditions within 7 min, while a HRR of 1000 kW requires only 2 min.

5. Combination of CFD and 0D model

Two parametric analyses can be performed, one to observe the effect of the pool dimension on the inlet heat flux using CFD, and one on the effect of the inlet flux on the possible runaway scenarios, for the determination of intervention times with the 0D model.

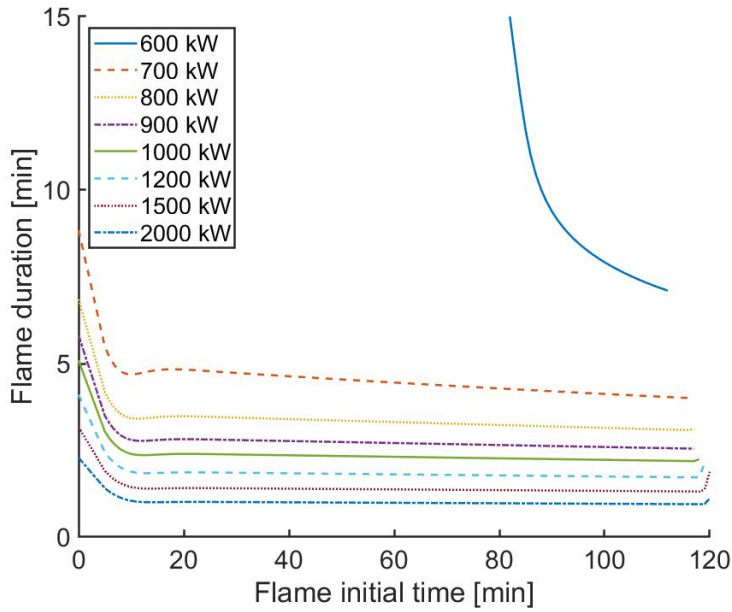


Figure 3: Flame duration needed to reach the MAT according to the time (within the process time) at which the flame starts engulfing the reactor for different values of the inlet power.

Figure 4 is therefore obtained. This figure allows, once a value of the pool fire is given, to estimate the power entering the reactor from the flame using the dashed line and the maximum intervention time using the dotted curve. For the sake of example, given a pool radius equal to 1.4 m on the left vertical axes (point A in Figure 4), we can identify at first the point B on the dashed line. From this point, the power entering the reactor can be easily read on the horizontal axes (about 1200 kW, point D in Figure 4). From the same point B, we can also identify point C on the dotted curve, from which the maximum intervention time can be read on the right vertical axes (about 2 min, point E in Figure 4).

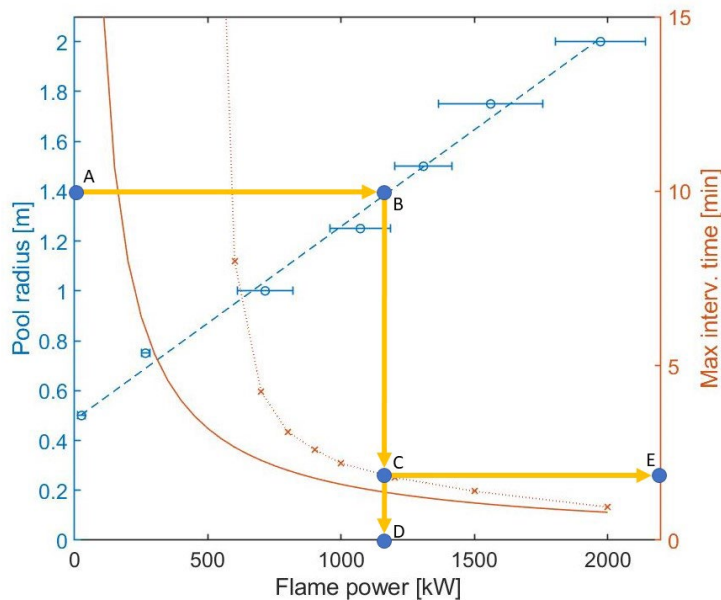


Figure 4: Combined results of the CDS analysis and the OD model, connecting the pool radius to the pool fire heat flux and consequently to the maximum intervention time. The dashed blue line is a linear fitting of the relationship between the pool radius and the flame heat flux; the solid red line is a simplified model for the determination of the maximum intervention time accounting only for sensible heating due to the flame in the absence of the external heat exchanger and no reaction.

Notably, the flame heat flux (dots, with an error bar computed from the standard deviation of the averaged total heat flux in the simulation) increases linearly with the pool radius and it is almost null for flames having a radius below 0.4 m, meaning that the flame cools down (due to the heat exchange with the environment) before reaching the bottom of the reactor. The plot reports the maximum intervention times (crosses) showing that for large heat fluxes the intervention time can be computed assuming a linear increase of temperature (neglecting reaction heat and external heat exchanger) as reported from the solid line (computed as $m_0 \tilde{c}_p \Delta T / \dot{Q}_f$, where ΔT is the temperature difference between the operating temperature, 180 °C, and the MAT). This limit behavior corresponds to conditions where the temperature increase due to the external fire acts on a time scale that is much lower than the reaction time and the duty of the heat exchanger is much lower than this power. For lower flame heat release rates, the intervention time becomes larger, thanks to the beneficial effect of the heat exchanger, up to a minimum flame heat flux (roughly equal to 500 kW) for which the intervention time becomes much larger than 30 min, meaning that any flame which has a HRR lower than 500 kW will provide an influx of heat that can be managed by the external heat exchanger.

6. Conclusions

A pool-fire accidental scenario, possibly triggering runaway in a process vessel as a domino effect, was studied for the case of an ethoxylation Venturi Loop Reactor. A CFD simulation of the pool fire (considering different pool dimensions) was able to determine the flame heat flux provided to the engulfed reactor and the degree of engulfment (total/partial). This result was then used within a simple 0D model of the internal part of the vessel, where the ethoxylation reaction occurs, together with the undesired decomposition of ethylene oxide (for which CFD modelling could be impractical because of the extremely turbulent conditions coupled with reaction in a multi-phase system). According to the value of the heat power provided by the flame, it was possible to observe whether the maximum allowed temperature can be exceeded, given the duration and initial time of the fire accidental scenario. The coupling of the CFD simulation and the 0D model predictions allowed to find a maximum intervention time (allowing the application of some automatic/active protection) according to the characteristic dimension of the pool fire.

References

- Copelli S., Derudi M., Rota R., Lunghi A., Pasturenzi C., 2011, Experimental Design of Topological Curves to Safely Optimize Highly Exothermic Complex Reacting Systems, *Industrial & Engineering Chemistry Research*, 50, 17, 9910–9917.
- Copelli S., Derudi M., Sempere J., Serra E., Lunghi A., Pasturenzi C., Rota R., 2011, Emulsion polymerization of vinyl acetate: Safe optimization of a hazardous complex process, *Journal of Hazardous Materials*, 192, 8-17.
- Crococ L., Glassman I., Smith I. E., 1959, Kinetics and Mechanism of Ethylene Oxide Decomposition at High Temperatures, *The Journal of Chemical Physics*, 31, 506-510.
- Di Serio M., Tesser R., Santacesaria E., 2005, Comparison of Different Reactor Types Used in the Manufacture of Ethoxylated, Propoxylated Products, *Ind. Eng. Chem. Res.*, 44, 9482-9489.
- Feldkamp M., Quercetti, T., Wille, F., 2020, Outcomes of three large scale fire reference tests conducted in bam fire test facility, *American Society of Mechanical Engineers, Pressure Vessels and Piping Division (Publication) PVP*, 8, art. no. v008t08a038.
- Florit F., Favrin S., Rota R., Derudi M., 2019, Jet fires and reaction runaway interaction: A multiscale approach, *Chemical Engineering Transactions*, 77, 367-372.
- Gonzalez F., Prabhakaran A., Robitaille A., Birk A.M., Otremba F., 2016, Rail tank car total containment fire testing: Results and observations, 2016 Joint Rail Conference, JRC 2016.
- McGrattan K., Hostikka S., McDermott R., Floyd J., Weinschenk C., Overholt K., 2013, *Fire Dynamics Simulator, Technical Reference Guide, Mathematical Model*, vol. 1, NIST Special Publication 1018.
- Scarponi G., Landucci G., Birk A.M., Cozzani V., 2019, CFD study of the fire response of vessels containing liquefied gases, *Chemical Engineering Transactions*, 77, 373-378.
- Scarponi G.E., Landucci G., Birk A.M., Cozzani, V., 2021, Three dimensional CFD simulation of LPG tanks exposed to partially engulfing pool fires, *Process Safety and Environmental Protection*, 150, 385-399.
- Tavelli S., Derudi M., Cuoci A., Frassoldati A., 2013, Numerical analysis of pool fire consequences in confined environments, *Chemical Engineering Transactions*, 31, 127-132.